Numerical modelling of skimming flow over small converging spillways

F. Nunes[1], J. Matos[2] and I. Meireles[3]

[1] WSP, Guildford, United Kingdom

[2] CERIS, Instituto Superior Técnico, Universidade de Lisboa, Lisbon, Portugal

[3] RISCO, Departamento de Engenharia Civil, Universidade de Aveiro, Aveiro, Portugal

Abstract

Recently, a significant number of embankment dams have been considered unsafe due to inadequate spillway capacity and predicted overtopping during extreme flood events. The use of stepped overlays for overtopping protection has proven to be cost effective and has gained acceptance worldwide, particularly in the USA. An interesting alternative configuration to the typical stepped spillway of constant width is the use of converging chute walls. This spillway typology enables the increase of the crest length in relation to the chute width at the toe, allowing a decrease of the head above the crest, for identical discharge, and complying with possible width constrains at its downstream end. However, a wall deflection induces undesired cross-waves by increasing the flow depths in the vicinity of the wall, which should be taken into account for design purposes.

This study presents a 3D numerical study using the Computational Fluid Dynamics (CFD) code FLOW-3D®, with simulations performed using a RANS approach coupled with the RNG k-ε turbulence modelling. Some main flow characteristics along the converging spillway, for smooth and stepped inverts, were evaluated and compared with those previously acquired on a physical model with a 1V:2H sloping chute, typical of the downstream slope of small embankment dams. The results show that, in general, a good agreement was found between numerical and experimental data along the nonaerated flow region, on both smooth and stepped inverts, namely regarding flow depths in the chute centreline and at the chute sidewalls, as well as velocity profiles in the chute centreline.

Keywords

Spillway chute, skimming flow, converging chute walls, CFD, FLOW-3D®

1 Introduction

Over the last decades, stepped spillways have become a popular overflow structure in dam engineering. The macro-roughness created by the steps enhances the energy dissipation along the chute, leading to a reduction of the size of the energy dissipator at the toe, and respective construction costs. The application of RCC stepped spillways for rehabilitation of small embankment dams may encompass non-conventional spillway geometries (Figure 1). This may be due to geological or topographical constraints, or those imposed by urban development, leading to the need for converging chutes, namely on stepped overlays (e.g., Hunt et al. 2008, 2012).

Figure 1. RCC overtopping protection of embankment dams: Yellow River Watershed Dam No. 14, USA, rehabilitated in 2004 (Photograph: J. Matos, March 2007).

Chute wall convergence increases the flow complexity, with the wall deflection inducing increased flow depths in the wall region, in comparison to those in the chute centreline.

In the last decades, extensive research has been carried out worldwide on the hydraulics of stepped spillways, embracing physical modelling or numerical studies (e.g., Hunt et al. 2014, Matos & Meireles 2014, Chanson et al. 2015, Frizell & Frizell 2015). However, a more limited number of theoretical and experimental studies have been conducted on the hydraulics of converging stepped spillways (e.g., André & Ramos 2003; Cabrita 2007; Hunt et al. 2008, 2012; Woolbright 2008; Zindovic et al. 2016), and fewer studies made use of CFD codes as a way to complement and support the analysis of this type of spillways (e.g., Lesleighter et al. 2008; Willey et al. 2010).

For a given stepped spillway, the flow pattern may be either nappe, transition, or skimming flow for increasing discharge (e.g., Chanson 2002; Matos & Meireles 2014). In the skimming flow regime, usually relevant for the design of RCC overtopping protection systems, the water skims over the step edges, whereas the step cavity is filled with circulating fluid.

Similarly to high-velocity flows on smooth spillways, skimming flow down stepped spillways can be divided into two regions: a clear-water flow region close to the spillway crest, where the boundary layer grows from the spillway floor and the water surface is quite smooth and glassy; and an air-water flow region downstream of the point of inception of air entrainment (e.g., Wood 1991, Chanson 1996). The point of inception of air entrainment moves downstream with increasing discharge, and much larger boundary layer growth occurs on stepped chutes in comparison to that observed on smooth channels (e.g., Chanson 1994, Matos & Meireles 2014). However, in the presence of moderate unit discharges on small dams, the boundary layer may not have a long enough distance to fully develop, and, consequently, air entrainment may not take place. Therefore, the study of the nonaerated flow properties may be relevant for hydraulic design purposes, particularly for small embankment dams.

In the present study, a 3D numerical study, with the CFD code FLOW-3D®, was applied to model the skimming flow on small smooth and stepped chutes with converging walls. Typical results of flow depth and velocity profiles were also compared with those previously acquired on a 1V:2H sloping physical model chute.

2 Experimental data

The experimental facility used for validation of the numerical model presented herein was assembled at the Laboratory of Hydraulics and Water Resources of the Instituto Superior Técnico (IST), in Lisbon.

The facility comprised an uncontrolled broad-crested weir followed by a chute and a stilling basin (Figure 2). The weir was 0.5 m long, 0.5 m high, and incorporated a semicircular upstream corner to reduce flow separation at the entrance. The slope of the chute was 1V:2H (26.6° from horizontal), and its width was 0.70 m. Experimental tests were conducted for skimming flow on constant width and/or converging chutes, namely by André & Ramos (2003) and Cabrita (2007).

The numerical study reproduced a configuration of symmetrical chute wall convergence with an angle (θ) of 9.9°, for three types of surface macro-roughness (Table 1, Figure 2). All tests on the stepped chutes corresponded to the skimming flow regime, for flow rates (Q) between 35 and 56 l/s, that is, unit discharges at the crest ranging between 0.05 and 0.08 m^2/s, respectively.

Further details on the experimental setup and instrumentation can be found in André & Ramos (2003), Cabrita (2007) and Meireles & Matos (2009).

Table 1. Roughness types tested in the surface of the chute.

Macro-roughness type	No. of steps
Smooth (PVC)	--
Steps with h =2.5 cm	20
Steps with h =5.0 cm	10

(a) (b)

Figure 2. Experimental facility with two converging chute walls (θ = 9.9°): (a) smooth chute (b) stepped chute, h = 2.5 cm (Cabrita 2007).

3 Numerical model

Reynolds Averaged Navier-Stokes equations (RANS) have been numerically solved by means of the finite volume method, coupled with RNG $k{-}\varepsilon$ turbulence modelling, being k the turbulent kinetic energy and ε the turbulent dissipation rate, both modelled by their respective transport equations (Yakhot et al. 1992). FLOW-3D® uses an advanced algorithm for free surface tracking, TruVOF, developed by Hirt & Nichols (1981), hence, it is simulated with one-fluid approach avoiding the need of modelling the air above the surface, treated as a moving boundary condition for air entrainment. After defining both geometry and a Cartesian, staggered grid, the software uses FAVOR™ method to incorporate geometry effects into the governing equations. The preprocessor, using this technique, generates area fractions for each cell face in the grid by determining which corners of the face are inside of a defined geometry and reconstructing the geometry based on these parameters (Flow Science, Inc., 2015). Therefore, the process is heavily dependent on the mesh resolution.

4 Numerical model implementation

4.1 Geometry and mesh

The solid geometry was generated component by component using the tools provided by FLOW-3D® in order to reduce possible resolution issues due to the application of FAVOR™ method. One of the configurations used as case-study is presented in Figure 3 (x, y and z are the longitudinal, transverse and normal coordinates, respectively).

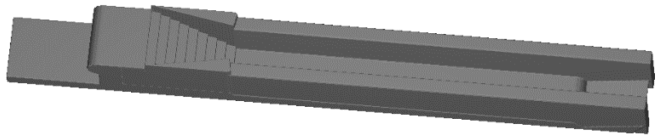

Figure 3. Geometry used in the numerical simulations for the stepped spillway with two converging chute walls (θ = 9.9°; h = 5.0 cm).

In this study, 3D simulations were performed. In order to reduce the computational time, a symmetry boundary condition was defined at $y = 0$ for the symmetric configuration, simulating only half of the domain. In a symmetry plane the shear stress is zero and the flux of properties across the boundary is not allowed, predicting the same flow conditions in the region immediately outside of the boundary and reducing significantly the computational time. Four different types of mesh were defined (Table 2). Meshes 2 and 4 are composed by two Cartesian blocks: block 1 is a coarse buffer mesh and the second mesh block, block 2, is nested inside the first, containing finer cells on the domain of interest (stepped chute region).

Table 2. Mesh types used for the spillway modelling with two converging chute walls (θ = 9.9°).

Mesh type	No. of cells	Cell size (m)
1	983 808	0.0125 x 0.0125
2	1 972 992	Block 1: 0.0125 x 0.0125 Block 2: 0.00625 x 0.00625
3	415 296	0.01667 x 0.01667
4	832 608	Block 1: 0.01667 x 0.01667 Block 2: 0.00833 x 0.00833

4.2 Boundary conditions

In block 1, the upstream boundary condition, x_{min}, was set as a specified pressure with definition of the fluid elevation as measured experimentally by Cabrita (2007). For the downstream boundary condition, x_{max}, an outflow condition was applied. For the symmetrical chute, y_{min} was set as a solid boundary condition (wall) and y_{max} was defined as a symmetry boundary condition. The bottom boundary (z_{min}) was defined as wall (no-slip condition) and the top boundary (z_{max}) was set with a specified pressure in which fluid fraction is zero and the pressure is equal to the atmospheric one (101325 Pa). In block 2, all boundary conditions were set as symmetry, with the exception of y_{min}, defined as a wall condition, and z_{max}, defined with the same condition (specified pressure) as for block 1.

4.3 Physics models

The activated physics models were: air entrainment, bubble and phase change, density evaluation, drift-flux, gravity and non-inertial reference frame and viscosity and turbulence. The chosen turbulence model was the RNG $k\!-\!\varepsilon$. The TLEN (maximum turbulent length scale) was set to be dynamically computed by the software, since it is also the most recommended option according to Flow Science, Inc. (2015). The air entrainment model, developed by Hirt (2003), was added with an entrainment rate coefficient of 0.5 and surface tension coefficient of 0.073 N/m, and with bulking and buoyancy options activated. For the numerical approximation of the advection terms, a first order scheme was employed for an initial period of time, followed by an explicit second order scheme with gradient preserving using a *Restart* simulation.

4.4 Mesh independence study

Mesh independence tests were conducted for Q = 35 l/s, with depths and velocities having been tracked over the different meshes presented in Table 2, for both step heights. In the nonaerated region of the stepped chute with h = 2.5 cm ($L \leq 0.56$ m), the mean relative differences between meshes 2 and 4 were 2.9% for the depths along the centreline (Figure 4) and 3.9% along the right wall. For a step height of 5.0 cm, those values were 3.4 and 3.8%, respectively. Therefore, a grid-independent solution was achieved in the nonaerated region of the spillway. However, an increasing difference in flow depths between meshes, including those more refined (i.e., meshes 2 and 4), was noticeable in the self-aerated region of the spillway (e.g., Figure 4, for L > 0.56 m).

The velocity profiles in the nonaerated region of the stepped chute showed similar values close to the free surface, but they were found to be sensitive to mesh size near the pseudo-bottom (in Nunes 2017).

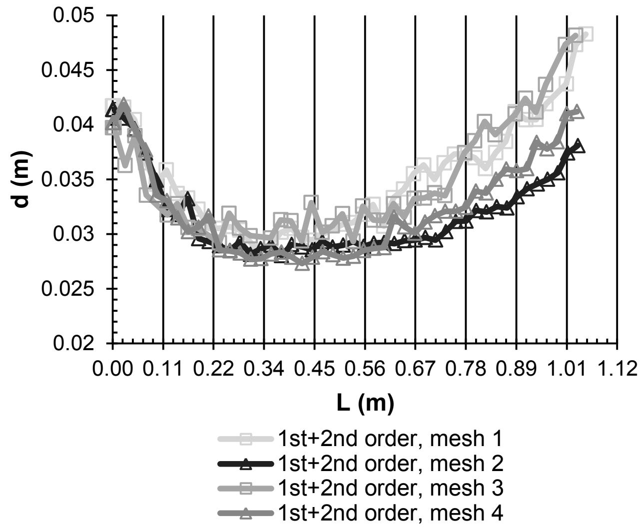

Figure 4. Numerical flow depths along the centreline for the stepped spillway with two converging chute walls (θ = 9.9°; h = 2.5 cm; Q = 35 l/s).

4.5 Simplified numerical model: symmetry boundary condition

Due to the computational time involving the meshes presented in Table 2, a simplification of the numerical model of the symmetrical spillway was used by imposing a symmetry condition and therefore allowing for a simulation of only half of the model. However, this boundary condition imposes certain features, such as null velocity in the normal direction of the boundary. A sensitivity analysis was conducted by comparing the modelling of the entire computational domain with half of it (Nunes 2017). The results showed that the model simplification had a very small influence on the numerical results of the flow depth in the nonaerated flow region. Even though considerably larger differences were observed for the velocity profiles in the nonaerated region near the point of inception, for the *Restart* simulation, the simplification of the symmetrical spillway was considered acceptable.

5 Results and discussion

5.1 Flow rate

Similarly to Lúcio (2015), flow rates were not an imposed condition in any of the boundaries. In order to evaluate if the flow rates obtained in the numerical simulations corresponded to those of the experimental tests, the relative differences between experimental and numerical discharges were evaluated (Table 3). Therein δ_1 and δ_2 refer to the relative differences between the experimental flow rate obtained by Cabrita (2007) and, respectively, the simulated flow rate on the upstream and downstream boundaries for the final time of the initial simulation. The values presented in Table 3 are for the symmetrical spillway with flow rates corresponding to half of the computational domain (model simplification).

Table 3. Relative differences between experimental and numerical values of the discharge at x_{min} and x_{max} boundaries.

$Q_{exp}/2$	$Q_{num}/2$ (x_{min})	$Q_{num}/2$ (x_{max})	δ_1	δ_2
(l/s)			(%)	
17.5	16.96	16.88	-3.1	-3.5
21.0	21.02	21.39	0.1	1.8
24.5	23.97	24.13	-2.2	-1.5
28.0	26.82	26.74	-4.2	-4.5

5.2 Flow properties along the stepped spillway

In this section, the experimental data and numerical results are presented for a flow rate of 56 l/s (unit discharge at the upstream end of the chute of 0.08 m^2/s). For such flow rate, nonaerated flow conditions occur along the entire chute length, regardless of the chute macro-roughness.

In Figure 5, experimental and numerical flow depths obtained at the chute centreline and at one converging sidewall are shown for smooth and stepped chutes. In the chute centreline, the numerical results are in general fairly close to the experimental counterparts, in particular for the smooth chute and for the stepped chutes, using first followed by second order numerical approximations of the advections terms. However, an overestimation of the flow depths is noticeable near the downstream end of the stepped chutes, namely for $L \geq 0.78$ m (Figures 5c, e).

With regard to the flow depths on the right wall of the spillway, the numerical results are also similar to the experimental data, except at the upstream end of the spillway ($L < 0.22$ m), regardless of the type of invert (smooth or stepped); in the vicinity of the slope change region, considerably lower flow depths were obtained from the numerical simulations.

The experimental values of the velocity measured by Cabrita (2007) were compared with the numerical counterparts for distinct types of chute macro-roughness. Figure 6 shows velocity profiles on the centreline of three cross-sections along each chute.

An overall good agreement was obtained between the numerical results and the experimental data on the smooth chute as well as on the stepped chutes (particularly using first followed by second order numerical approximations of the advections terms), but close to the pseudo-bottom, where larger relative differences were found on the stepped chutes (e.g., Figures 6e, f). Both numerical and experimental results show the influence of the stepped macro-roughness on the decrease of the velocity in the inner flow region, in comparison to that obtained in the smooth chute. In the vicinity of the free-surface, the velocity is less dependent on the macro-roughness, as expected, because the boundary layer is developing and has not reached the free-surface.

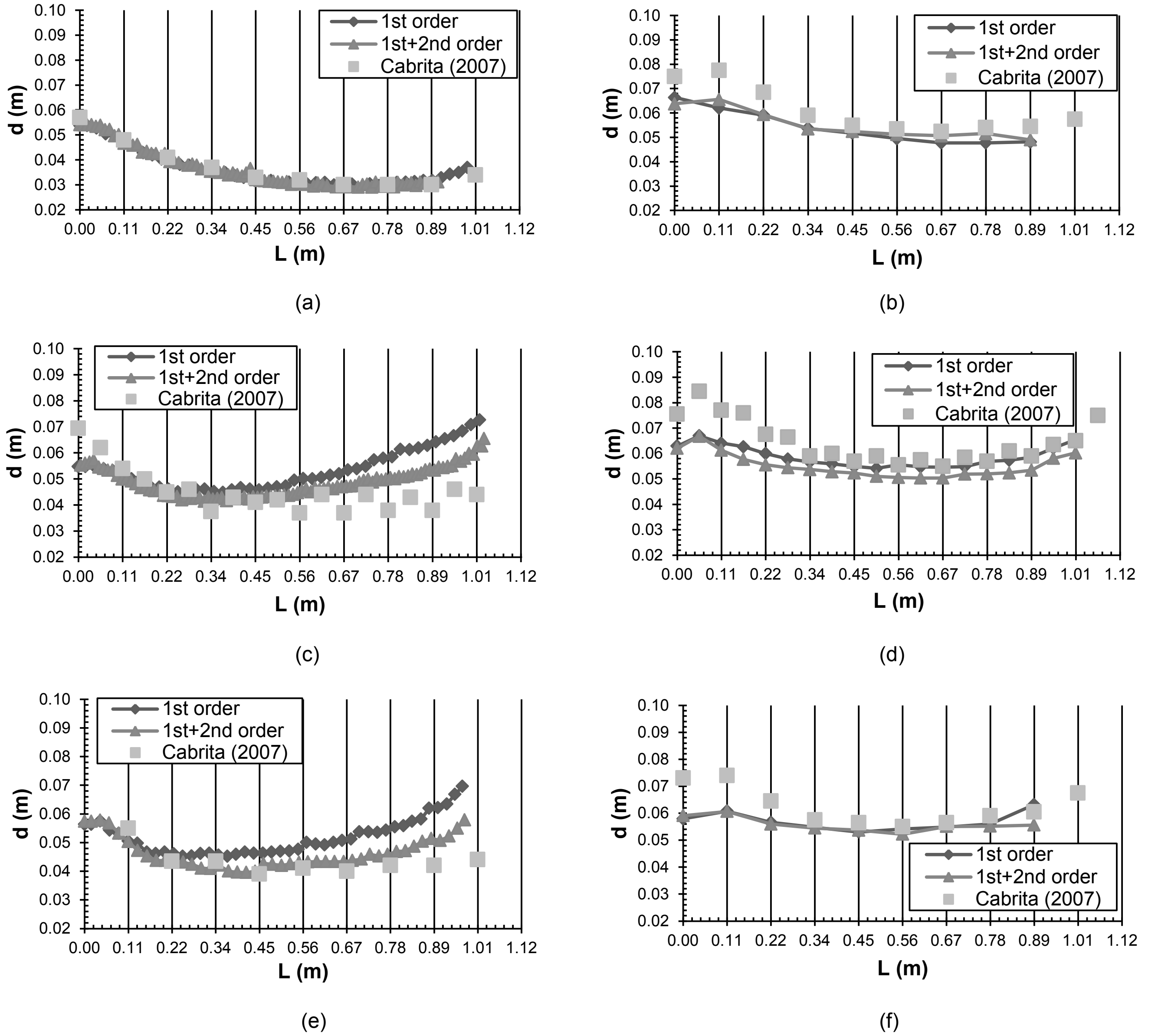

Figure 5. Experimental and numerical flow depths along the 9.9° converging chute, for Q = 56 l/s and mesh 4: (a) smooth chute, centreline; (b) smooth chute, converging wall; (c) stepped chute (h = 2.5 cm), centreline; (d) stepped chute (h = 2.5 cm), converging wall; (e) stepped chute (h = 5 cm), centreline; (f) stepped chute (h = 5 cm), converging wall.

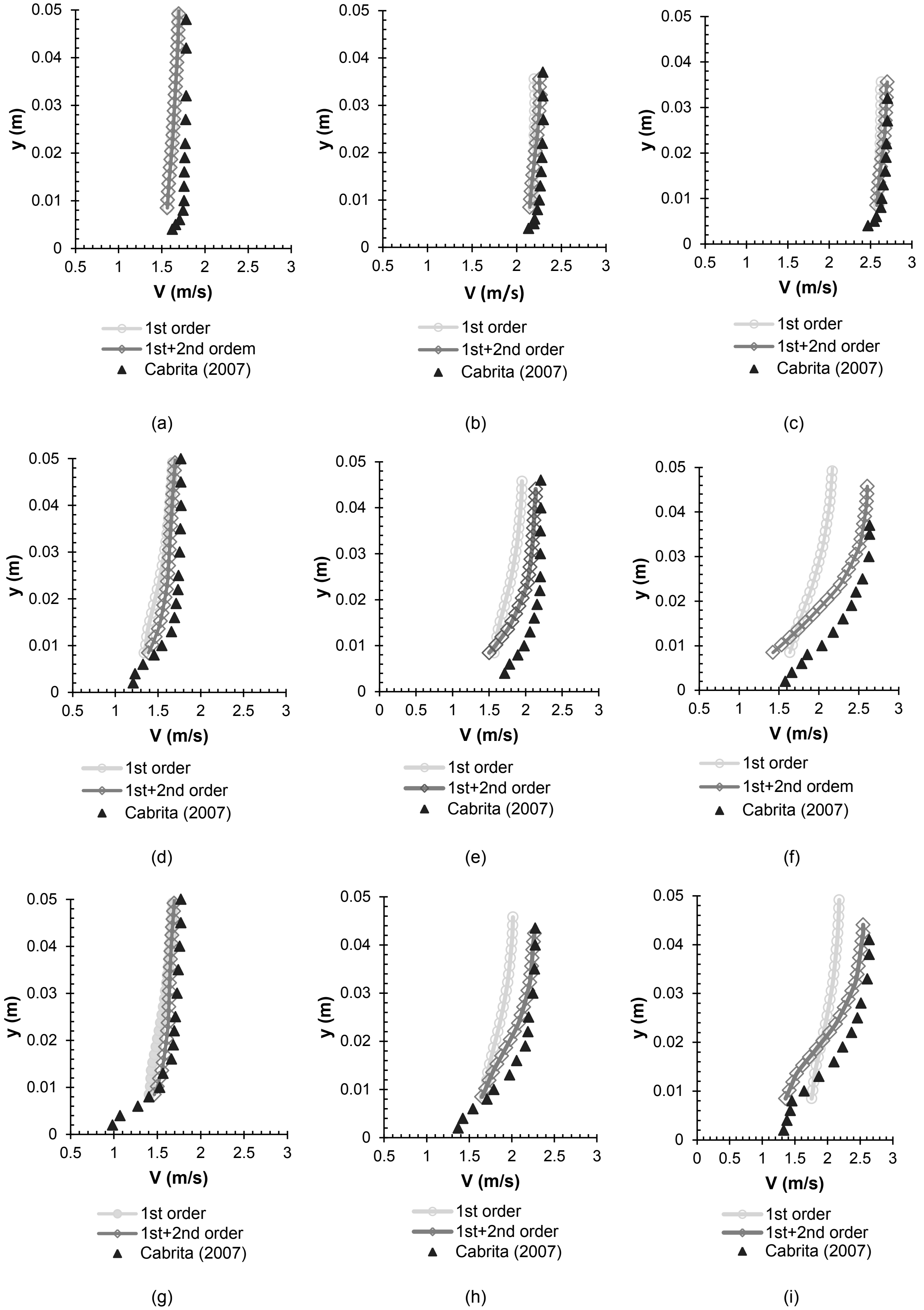

Figure 6. Experimental and numerical velocity profiles on the centreline of the 9.9° converging chute, for Q=56 l/s: (a) smooth chute, L = 0.11 m; (b) smooth chute, L = 0.34 m; (c) smooth chute, L = 0.56 m; (d) stepped chute (h = 2.5 cm), L = 0.11 m; (e) stepped chute (h = 2.5 cm), L=0.34 m; (f) stepped chute (h = 2.5 cm), L=0.56 m; (g) stepped chute (h=5.0 cm), L=0.11 m; (h) stepped chute (h=5.0 cm), L=0.34 m; (i) stepped chute (h= 5.0 cm), L=0.56 m.

6 Conclusions

In the present study, a 3D numerical study with the CFD code FLOW-3D®, was applied to model the skimming flow on small smooth and stepped converging spillways. Typical results of flow depth and velocity profiles were compared with those previously acquired on a 1V:2H sloping chute, for 9.9° converging walls.

In general, the numerical results of flow depths and velocity profiles at the chute centreline were fairly close to the experimental counterparts, for the smooth and stepped chutes, namely if a first order scheme followed by an explicit second order scheme was used for the numerical approximation of the advection terms. However, a tendency of overestimation of the flow depths on the chute centreline was noticeable near the downstream end of the stepped chutes, and the opposite was verified in a short reach near the upstream end of the chute. In addition, the fit of the velocity profiles in the inner flow region was less satisfactory.

As expected, the smooth spillway showed in general a better agreement between the experimental and numerical results, which would be expected, due to the reduced complexity of the flow near the invert, when compared to that of the stepped chutes.

References

André, M & Ramos, P 2003, Hidráulica de descarregadores de cheia em degraus e aplicação a descarregadores com paredes convergentes. Research Report, Instituto Superior Técnico, Lisbon (in portuguese).

Cabrita, J 2007, Caracterização do escoamento deslizante sobre turbilhões em descarregadores de cheias em degraus com paredes convergentes. M.Sc. thesis, Instituto Superior Técnico, Lisbon (in portuguese).

Chanson, H. 1994, *Hydraulic design of stepped cascades, channels, weirs and spillways*, Pergamon, Oxford, UK.

Chanson, H. 1996, *Air bubble entrainment in free surface turbulent shear flows*, Academic Press, London.

Chanson, H 2002, *The hydraulics of stepped chutes and spillways*, Balkema, Lisse, The Netherlands.

Chanson, H, Bung, D & Matos, J 2015, *Stepped spillways and cascades*, in Energy Dissipation in Hydraulic Structures. IAHR Monograph, CRC Press, Taylor and Francis Group, Leiden, The Netherlands, H. Chanson Editor, pp. 45-64.

Flow Science, I 2015, *FLOW-3D User's Manual. Version 11.1*. New Mexico, USA.

Frizell, KW & Frizell, KH 2015, *Guidelines for hydraulic design of stepped spillways*, Hydraulic Laboratory Report HL-2015-06, Bureau of Reclamation, U.S. Dept. of the Interior, Denver, Colorado, USA.

Hirt, CW 2003, *Modeling turbulent entrainment of air at a free surface*. Flow Science, Inc., Technical Note 61 FSI-03-TN61.

Hirt, CW & Nichols, BD 1981, 'Volume of fluid (VOF) method for the dynamics of free boundaries', *Journal of Computational Physics*, 39, pp.201–225.

Hunt, SL, Temple, DM, Abt, SR, Kadavy, KC & Hanson, G 2012, 'Converging stepped spillways: simplified momentum analysis approach', *Journal of Hydraulic Engineering*, vol. 138, no. 9, pp.796–802.

Hunt, SL, Kadavy, KC & Hanson, GJ 2014. 'Simplistic design methods for moderate-sloped stepped chutes', *Journal of Hydraulic Engineering*, vol. 140, no. 12: 04014062-1-15

Hunt, SL, Kadavy, KC, Abt, SR & Temple DM 2008, 'Impact of converging chute walls for roller compacted concrete stepped spillways'. *Journal of Hydraulic Engineering*, vol. 134, no. 7, pp.1000–1003.

Lesleighter, E, McPherson B, Riddette K & Williams J 2008, 'Modelling procedures used for the spillway upgrade for Lake Manchester Dam', *In ANCOLD Proceedings of Technical Groups: Dams and Water for the Future*.

Nunes, F 2017, Modelação computacional do escoamento deslizante sobre turbilhões em descarregadores de cheias em degraus com paredes convergentes. M.Sc. thesis, Instituto Superior Técnico, Lisbon (in portuguese).

Lúcio, I 2015, Modelação numérica do escoamento deslizante sobre turbilhões em descarregadores de cheias em degraus: aplicação a pequenas barragens de aterro. M.Sc. thesis, Instituto Superior Técnico, Lisbon (in portuguese).

Meireles, I, & Matos, J 2009, 'Skimming flow in the non-aerated region of stepped spillways over embankment dams', *Journal of Hydraulic Engineering*, vol. 135, no. 8, pp. 685–689

Matos, J & Meireles, I 2014, 'Hydraulics of stepped weirs and dam spillways : engineering challenges, labyrinths of research', *Proceeding of the 5th International Symposium on Hydraulic Structures. Hydraulic Structures and Society: Engineering Challenges and Extremes*, 25-27 June. Brisbane, Australia.

Willey, J, Ewing, T, Lesleighter, E & Dymke, J 2010, 'Numerical and physical modelling for a complex stepped spillway', *Hydropower & Dams*, Issue Three, pp. 103–113.

Wood, IR 1991, *Free surface air entrainment on spillways*, in Wood, IR Air entrainment in free surface flows, IAHR, Hydraulic Structures Design Manual 4, Hydraulic Design Considerations, A.A. Balkema, Rotterdam, The Netherlands, pp. 55–84.

Woolbright, R 2008, Hydraulic performance evaluation of RCC stepped spillways with sloped converging training walls. M.Sc. Thesis, Oklahoma State University, USA.

Yakhot, V, Orszag, SA, Thangam, S, Gatski, TB & Speziale, CG 1992, 'Development of turbulence models for shear flows by a double expansion technique', *Physics of Fluids A: Fluid Dynamics*, vol. 4, no. 7, pp.1510–1520.

Zindovic, B, Vojt, P, Kapor, R & Savic, L 2016, 'Converging stepped spillway flow', *Journal of Hydraulic Research*, vol. 58, no. 2, pp. 699–707.